

Preparation and In vitro/Ex vivo Evaluation of Nanoemulsion-Based *in Situ* Gel for Intranasal Delivery of Lasmiditan

Saba Abdulhadi Jaber^{*,1} and Nawal Ayash Rajab¹

¹Department of Pharmaceutics, College of Pharmacy, University of Baghdad, Baghdad, Iraq.

*Corresponding author

Received 9/6/2023, Accepted 12/9/2023, Published 15/9/2024



This work is licensed under a Creative Commons Attribution 4.0 International License.

Abstract

Lasmiditan (LSM) was first authorized by the Food and Drug Administration in October 2019 for migraine headache termination without causing vasoconstriction due to its high agonist activity at the five hydroxy tryptamine subclass 1F (5HT1F) receptor site. LSM was formulated as a nanoemulsion-based *in situ* gel (NIG) to improve its oral bioavailability via application intranasally. We determined the solubility of LSM in oils, emulsifiers, and co-emulsifiers to identify the nanoemulsion (NE) components. Using Oleic acid (OA), Labrasol® (LR), Transcutol® (TC), and deionized water (DD), a phase diagram was developed to identify the nano-emulsification region. The spontaneous nanoemulsification method was used to formulate LSM as NE. Based on these constructed pseudo-ternary phase diagrams, twenty different NE formulations were developed, then analyzed visually and subjected to a study of their thermodynamic stability, droplet size, polydispersity index (PDI), drug content, as well as *in vitro* release; all were measured to predict the optimum formulations. Four NEs (F1, F6, F13, and F16) containing 7-15% OA as an oily phase, 40-55% LR, and TC as emulsifier mixture at (1:1), (2:1), (3:1), and (1:2) ratios with 30-53% (w/w) aqueous phase, having suitable optical transparency of 95-98%, droplet size of 104-140 nm, and PDI of 0.253-0.382 were selected for an *ex vivo* permeation study. F13 has the highest flux value (2.32 ± 0.01 mg/cm².min) relative to the other NEs, so it achieves an enhancement ratio of 3.3 as compared to LSM aqueous suspension (8% LSM), and it also achieves a significantly higher value of permeability coefficient. F13 was selected to incorporate different percentages of pH-sensitive *in situ* gelling polymer (Carbopol 934) to prepare NIGs I, II, and III. The gel strength, pH, gelation capacity, and viscosity were predicted for the prepared NIGs. *In vitro* release and *ex vivo* nasal permeation were determined for NIG-II. It has a longer residence duration than F13 but the same release and permeation values to surpass the ordinary physiological clearance in the nose. As a conclusion of the previous work, NIG-II is considered a promising drug delivery system for LSM because it improves its poor oral bioavailability and achieves rapid onset of action.

Keywords: *Ex-vivo* permeation study, Nanoemulsion, Intranasal, *in situ* gel, and Lasmiditan.

التحضير والتقييم في المختبر/خارج الجسم الحي للجل الموضعي المستند إلى مستحلب النانو لتوصيل اللاسميديتان عبر الأنف

صبا عبد الهادي جابر^{*,1} و نوال عياش رجب¹

¹ قسم الصيدلانيات، كلية الصيدلة، جامعة بغداد، بغداد، العراق.

الخلاصة

تمت صياغة دواء اللازميديتان كمستحلب نانوي في الموقع بهدف تحسين التوافر البيولوجي عبر الفم عن طريق التطبيق داخل الأنف. تم تحديد قابلية ذوبان اللازميديتان في الزيوت والمواد اللتي تقلل الشد السطحي والمواد المساعدة على تقليل الشد السطحي لتحديد مكونات المستحلب النانوي. تم إنشاء مخططات الطور لتحديد منطقة استحلاب النانو. تمت صياغة دواء اللازميديتان كمستحلب نانوي باستخدام طريقة الاستحلاب النانوي العفوي. اربعة من الصيغ التركيبية المحضرة كمستحلب نانوي (F1, F6, F13, and F16) تحتوي على 7-15% (وزن / وزن) حمض الأوليك (OA) كمادة زيتية ، 40-55% (وزن / وزن) لابراسول (LR) ، و ترانسكيوتول (TC) كمزيج مستحلب بنسبة (1 : 1) ، (1 : 2) ، (1 : 3) ، و (2 : 1) مع 30-53% (وزن / وزن) طور مائي ، فكانت التراكيب المحضرة بشفافية بصرية مناسبة 95-98% ، حجم كروي من 104-140 نانومتر والتشتت المتعدد من 0.253-0.382 ، ولذلك تم اختيارهم لدراسة النفاذ خارج الجسم الحي. F13 مع أعلى قيمة للنفاذية (2.32 ± 0.01 ملغم/سم².دقيقة) بالنسبة إلى المستحلبات النانوية الأخرى. يحقق نسبة تعزيز تبلغ 3.3 مقارنة بالمعلق المائي لدواء اللازميديتان (8% لازميديتان) كما أنه يحقق قيمة أعلى بكثير لمعامل النفاذية. تم اختيار F13 لدمج نسب مختلفة من بوليمر التبلور الحساس للأس الهيدروجيني في الموقع (كاربوبول 934) لتحضير مستحلبات نانوية تتحول إلى جل في الموقع تحت مسمى NIGs I, II, and III. تم التنبؤ بقوة الهلام ، ودرجة الحموضة ، ووقت التكون ، واللزوجة للتركيبات المحضرة. تم تحديد نفاذية الأنف في المختبر وخارج الجسم الحي للتركيبية NIG II ، والذي يمارس قيم إطلاق وتغلغل مماثلة مثل F13 مع وقت إقامة أطول من أجل التغلب على التصفية الفسيولوجية للأنف الطبيعية.

الكلمات المفتاحية: دراسة التغلغل خارج الجسم الحي، المستحلب النانوي، الجل داخل الأنف، الجبل الموضعي، واللازميديتان.

Introduction

It wasn't until October 2019 that the Food and Drug Administration officially authorized the oral medication lasmiditan (LSM) for migraine headache relief ⁽¹⁾. The poor selectivity of earlier versions of five hydroxy tryptamine agonists (5HT) seems to be attributable, in large part, to the adverse effect profile that was not familiar to the new medication LSM works as a very selective agonist of the 5-HT_{1F} receptor site, and has almost little affinity for others. This selectivity enables the effective cessation of migraines without inducing constriction of blood vessels ⁽²⁾. It has been discovered that the oral bioavailability of LSM is approximately 40% ⁽³⁾. Due to its significant hepatic and extra-hepatic metabolism in humans, primarily by non-Cytochrome-mediated ketone reduction, and its role as a substrate for P-glycoprotein, LSM has poor oral bioavailability ^(4,5).

Because of their numerous potential advantages, such as avoiding hepatic first-pass metabolism and gastrointestinal degradation, increasing bioavailability at a reduced dose, simplifying administration, and rapid uptake into the body's bloodstream, formulation scientists have found the development of compounds that are nasally administered appealing ⁽⁶⁾. An increase in the drug's contact time in the nasal cavity may be the solution to the primary problem with this route of medicine delivery, which is mucociliary clearance.

More recently, formulations based on lipids have demonstrated the potential for improving the bioavailability of medications. Liposomes, lipid nanocarriers, microemulsions, NEs, oils or surfactant dispersions, and other methods are utilized for medication administration ⁽⁷⁾.

NE is an isotropic, clear, thermodynamically unstable, and kinetically stable dispersion system prepared with a water phase, an oil phase, an emulsifier, and a co-emulsifier. It has the advantages of small particle size, high solvent capacity, and excellent stability. The solubility of poorly soluble drugs can be increased via formulation as NE, and it also carries drugs with different solubilities, achieving synergistic effects between drugs and prolonging their effect ⁽⁸⁾.

The direct nasal administration of NE may cause leakage or irritation to the nasal mucosa. Therefore, the use of nasal NE-based in situ gel (NIG) in this research can effectively avoid or reduce mucociliary clearance and prolong the retention time of the drug on the nasal mucosa. Also, NIG promotes the dissolution and penetration of drugs in the nasal mucosa, reduces drug drips into the back of the throat, and improves the rate and extent of drug absorption ⁽⁹⁾. Many drugs with low

oral bioavailability, like Clozapine and tizanidine, were formulated as NE and incorporated into an in-situ gelling system to solve this problem ^(10,11).

Recent developments in the hydrogel drug delivery field include in situ systems, which are aqueous solutions in liquid form before administration but change into gels under physiological conditions ⁽¹²⁾. Carbopol 934 is the most widely used pH-induced gelling agent since it slows the body's natural excretion while extending the drug's stay on the nasal mucosa ^(13,14).

The objective of this work was to utilize nanotechnology to formulate LSM as a nasal NIG to provide a solution to the significant problems associated with the marketed LSM tablet, which include poor oral bioavailability and delaying the onset of action.

Materials and Methods

Materials

Lasmitane (LSM) was purchased from Yongchi Chemical Technology Co, LTD, China, Labrafil[®]M1944, Labrafac[®], Labrasol[®] ALF, isopropyl myristate, and Transcutol[®] were purchased from Gatte fosse (France). Imwitor[®]988 and Miglyol[®]812 N were purchased from IOI Oleochemical, GmbH, Germany. Oleic acid, Triacetin, Propylene glycol (PG[®]), and Carbopol 934 were purchased from Central Drug House. Castor, Olive, and sesame oils were purchased from Now Food, USA. Potassium dihydrogen phosphate and Di sodium hydrogen phosphate, Polysorbate (Tween[®]) 20, 40, 60, 80, Sorbitan monolaurate, Sorbitan monooleate (Span[®]) 20, 80, Polyethylene glycol (PEG[®]) 200, 300, 400, 600 all were purchased from Hi Media Laboratories Pvt Ltd, India.

Methods

Solubility studies

A shake flask technique was used to ascertain the solubility of LSM in different oils (Labrafac, Labrafil- M1944, Miglyol812, isopropyl myristate, Imwitor988, Oleic acid (OA), Castor oil, Sesame oil, Olive oil, and Triacetin), emulsifiers (Sorbitan monolaurate, Sorbitan monooleate, Polysorbate 20, 60, 40, 80, Labrasol[®] (LR)), and co-emulsifiers (Transcutol[®] (TC), Polyethylene glycol (PEG) 200, 300, 400, 600, and Propylene glycol (PG)). In each stoppered glass cylindrical tube holding, 2 ml of the chosen oils, emulsifiers, or co-emulsifiers, together with extra LSM (pure drug powder) which was added and mixed. The glass tubes were incubated at 25 ± 0.5°C in an isothermal shaker for three days. After incubation, the samples were centrifuged for 15 minutes at 3500 rpm before filtering via a Millipore (0.45 µm) filter syringe. Using an Ultraviolet Spectrophotometer, the filtrate was examined at λ 256 nm after being diluted with methanol ⁽¹⁵⁾.

Construction of phase diagram (PTD)

A phase diagram was developed to describe the scope and characteristics of the NE zones. The spontaneous nanoemulsification technique was used to create phase diagrams at room temperature. Depending on the solubility studies, OA, LR, and TC were used to prepare the NEs as the selected oil, emulsifier, and co-emulsifier, respectively. LR and TC were mixed at constant weight ratios (1:1, 2:1, 3:1, and 1:2 w/w) to create the phase diagram. Then, OA was added to each S-mix at ambient temperature. The oil-to-S-mix ratio was changed from 9:1 to 8:2, 7:3, 6:4, 5:5, 4:6, 3:7, 2:8, and 1:9 (w/w) for each phase diagram. Each oil-S-mix was stirred vigorously while water was dropping slowly. The samples were clear/transparent upon visual inspection upon equilibrium. The NE demonstrating phase separation appears visually turbid or gel-like, so it is not accepted⁽¹⁶⁻¹⁸⁾. It was determined where each S-mix produced NE with the ideal droplet size and stability.

Preparation of NE formulations

Using a water titration technique in line with PTD, a variety of O/W NE formulations have been developed, as shown in Table 1. 10 grams of 8% LSM NE were obtained by dissolving 0.8 grams of LSM in a mixture of OA (the chosen oil based on the solubility study) and an appropriate ratio of S-mix (LR and TC), which were both weighed before being stirred continuously on the magnetic stirrer at room temperature (500 rpm) for ten minutes⁽¹⁹⁾. Deionized water was added gradually while stirring constantly to get a clear NE⁽²⁰⁾. To create nanosized droplets, the manufactured NEs were passed through a Probe-Sonicator at 20 HZ for 2 minutes only⁽²¹⁾. Each step is depicted in great detail in Figure 1. The NEs were transferred to the new glass cylinder and kept at four °C in the refrigerator. The derived final formulas (F1–F20) underwent Optimization followed by characterization.

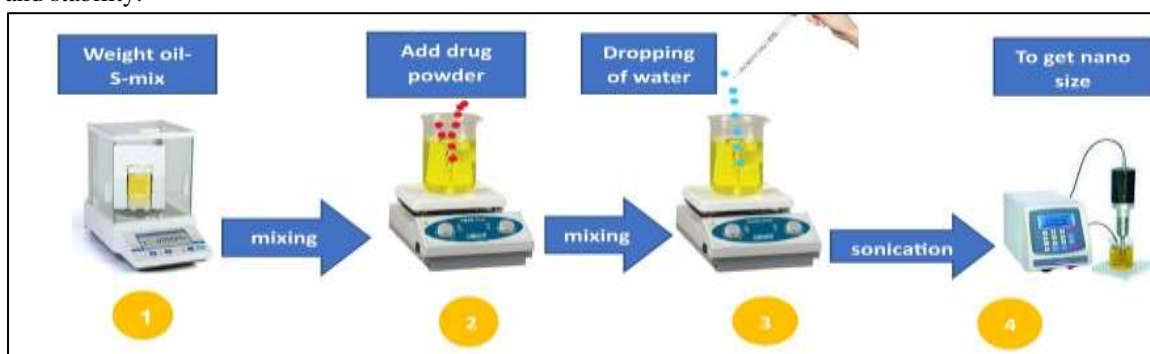


Figure 1. A schematic diagram describing the preparation of LSM NE using the water titration method.

Table 1. Major Constituents of LSM NE.

NE F-Code	Oleic Acid %	S-mix Ratio	S-mix %	DD %
F1	7	1:1	40	53
F2	10	1:1	50	40
F3	15	1:1	50	35
F4	20	1:1	52	28
F5	25	1:1	55	20
F6	7	2:1	40	53
F7	10	2:1	40	50
F8	15	2:1	55	30
F9	20	2:1	55	25
F10	25	2:1	55	20
F11	7	3:1	40	53
F12	10	3:1	45	45
F13	15	3:1	55	30
F14	20	3:1	55	25
F15	25	3:1	55	20
F16	7	1:2	53	40
F17	10	1:2	50	40
F18	15	1:2	50	35
F19	20	1:2	55	25
F20	25	1:2	50	25

*For all the prepared NEs (F1- F20), 8g of LSM was added to each formula, and % represents (W/W).

Thermodynamic stability studies

The produced NEs should be stable enough to pass thermodynamic stability tests before being optimized as NE formulations. All the NEs that did not show phase separations were subjected to heating and cooling experiments (H&C) after being centrifuged (CEN) for 30 minutes at 3500 rpm. Three freeze-thaw cycles (F-T) were performed on these formulations, with Temp ranging from -20 to +25°C. Physical characterization was applied to NE formulations after they passed the previous test (22,23).

Measurement of the PDI and droplet size

The NE formulations' droplet size and PDI were assessed using a Zeta sizer (UK). Half milliliters of each combination were diluted with 10 milliliters of DD, and each formulation's expected average droplet size and PDI were measured (24).

Percentage transmittance (T%)

The ultraviolet and visible spectrophotometer used to measure the % transmittance was a UV-1700 Pharma Spec model made by Shimadzu in Japan. The formulation was tested at 650 nm after being diluted one hundred times with DD, which was used as the reference material (25).

Dilution test.

The purpose of this experiment was to observe the phase inversion of the NE. One milliliter of tailored NE was mixed with ten milliliters of DD in a test tube. (26).

Drug Content Measurement

Initially, the NE formulation was diluted with methanol in a volumetric flask and then filtered using a Millipore (0.45 µm) filter syringe. The LSM NEs' content was assessed at the designated λ max, 256nm, utilizing an ultraviolet-visible spectrophotometer-1700, made in Japan (27).

In vitro release study

An artificial dialysis bag with a molecular weight of (8-14) k Da, which was previously soaked in a phosphate buffer solution (PBS) at pH 7.4, and a 0.25 g sample of each NE formula (F1-F20), pure drug (8% LSM aqueous suspension) and NIG. Each component was incorporated with the bag, which was then tied to the basket and immersed in the dissolution jar containing 100 ml of PBS at pH 7.4. with temperature maintained at 37°C. A maximum of two hours was spent agitating the mixture at 50 rpm. Samples of 2 ml were taken from the dissolution jar at various intervals and subsequently examined spectrophotometrically at 256 nm (28,29).

Ex vivo drug permeation studies

Fresh nasal tissue was carefully taken from the nasal cavities of sheep provided by the nearby butcher, rinsed in PBS at pH 6.4, and mounted on the Franz diffusion cell with a permeation area of 1.76 cm² between the donor and receptor compartments. Eleven milliliters of PBS, at pH 7.4, were poured into the receptor chamber (30). After a 20-minute pre-incubation period, separate additions

of 0.25 g of NE, NIG, and aqueous drug suspension (8% LSM suspended in DD) were made. The contents of the receptor chamber were continually stirred at 400 rpm using the magnetic bar. Over three hours, 0.5 ml samples were taken at regular intervals and analyzed spectrophotometrically at 256 nm to determine the LSM concentration (14,31). The results were expressed as the amount that reached the receptor chamber via a particular surface area (Q-value) versus time (32).

In-situ gel formulation.

The NE was produced as an *in-situ* gel with concentrations of 0.2, 0.5, and 0.7% after it passed all the previously listed tests. Once the chosen NE formula's components OA, LR, and TC were thoroughly weighed and mixed to create a uniform, transparent yellow solution, on the other hand, Carbopol 934 (a pH-induced *in situ* gel polymer) was sprinkled over the water content of the NE, left to hydrate overnight. Then a slow, steady drop was made over the transparent yellow mixture while stirring continuously at 500 rpm to obtain NIG I, II, and III, respectively, with Carbopol 934 conc (33).

Evaluation of in situ gels

pH of the in-situ gel

A handheld pH -meter called a Mico Matic was used to determine the pH of the prepared nanoemulsion *in situ* gel (NIG I, NIG II, and NIG III) after being calibrated with a standard buffer.

Gelation studies

In a glass cylinder tube, one milliliter of each NIG was mixed with one milliliter of artificial nasal fluid (ANF) at pH 6.4. The ANF contained 7.45 g/L of sodium chloride, 1.29 g/L of potassium chloride, and 0.32 g/L of calcium chloride. A water bath was used to keep the entire apparatus at a temp of 37± 1°C. Twenty seconds later, we switched the tubes around. Regarding visual evaluation, a formulation was given a "+" for gelation if it stuck to the inside of the tube and didn't slide down. This evaluation considered both gelation's start and disappearance times (14,34).

Gel strength measurement

ANF at pH 6.4 was used to neutralize a five-gram sample of each NIG, which was placed in a small cylinder and kept at 37°C by placing the cylinder on a hot plate. A 3.5 g weight was placed on top of the gel. The time required was measured in seconds to determine how long it took for the weight to penetrate three centimeters into the nasal *in situ* gel (35).

The measuring of viscosity

The information concerning the apparent viscosity was gathered using the fourth spindle of the Brookfield digital viscometer. For thirty seconds at 6, 12, 30, and 60 rpm, the NEIGs' viscosity was measured. It was done both before and after gelation (36,37).

Nanoemulsion surface morphology using TEM

Using a transmission electron microscope (TEM), the NE's surface morphology was analyzed to determine the best possible formulation. Before examining the NE, one drop of 2% w/v phosphotungstic acid water solution was inserted in the copper grid ^(38,39).

Statistical Analysis

Means and standard deviations (mean ± SD) were used to express the outcomes of the studies, which were repeated three times. To find out if there were any significant differences between the groups when comparing their mean values, one-way analysis of variance (ANOVA) was employed; p-

values were deemed significant at a level of (P< 0.05) and non-significant at a level of (p > 0.05).

Results and Discussion

Studies on solubility

Figure 2 from the Solubility Studies shows the relative amounts of LSM soluble in different oils, emulsifiers, and co-emulsifiers. According to the findings, OA and LR are suitable oils and emulsifiers for dissolving 32 and 31.4 mg/ml of LSM, respectively. With a considerable solubilizing activity (62.3 mg/ml), TC was used as a co-emulsifier to increase the drug loading capacity.

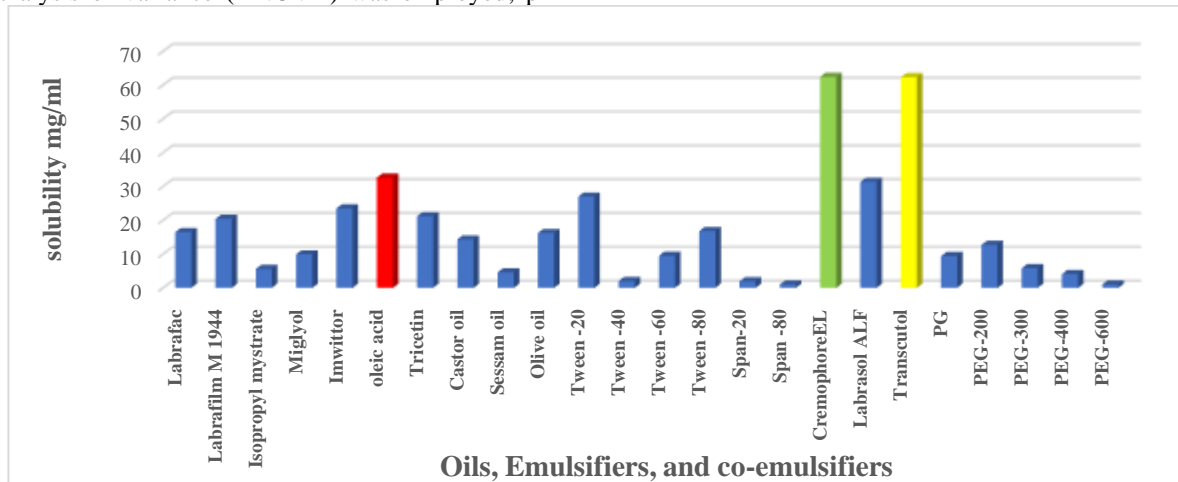


Figure 2. A visual depiction of the solubility of LSM in different oils, emulsifiers, and co-emulsifiers.

Pseudo-ternary phase diagram (PTD)

A PTD is a helpful tool for learning how the components of a mixture affect its phase behavior. Figure 3 shows the four ternary phase systems that

were produced by using the (LR: TC) with different mass ratios: 1:2, 3:1, 2:1, and 1:2. The shaded areas depict the NE, while the unshaded zone shows the multiphase emulsion.

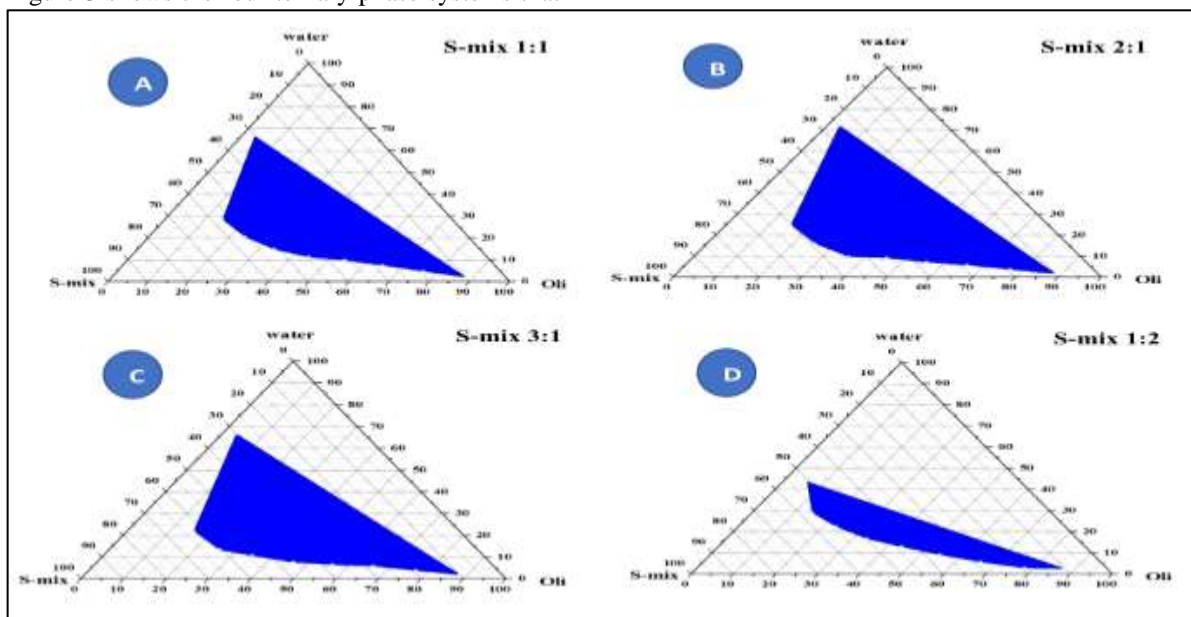


Figure 3. Schematics depicting the pseudo-ternary phase relationships of the OA, LR: TC (S-mix), and water system at different weight ratios of S-mix at room temperature.

A particular concentration of oil, S-mix, and water must be blended to create NEs, which are

thermodynamically unstable systems. The NE regions were enhanced when there was a higher LR

concentration as in the S-mix (2:1 or 3:1). The possible explanations declared that less interfacial tension leads to improved interface fluidity and deep oil phase penetration of the hydrophobic LR area (40,41). The highlighted region in each PTD was used to derive five distinct formulas, as shown in Table 1.

Thermodynamic Stability Studies

Studies on the thermodynamic stability of each produced NE formulation were completed. According to Table 2 data, all produced NEs did not exhibit any signs of phase separation, cracking, or a change in odor or color, except for F3, F7, F12, and F18(42).

Nanoemulsion characterization

Droplet size measurement and polydispersity index (PDI).

All nanosized particles made up the NE. The findings presented in Table 3 demonstrated that, for all S-mix ratios, droplet size increased with oil content (43).

High emulsifier ratios stabilize and condense the interfacial layer, and when the concentration of co-emulsifier rises, it will expand (44).

The co-emulsifier molecules possibly permeating the emulsifier coating cause the small mean droplet size. As a result, the interfacial layer's surface may be reduced, leading to droplets with decreased radii of curvature and the development of transparent systems. As an outcome, droplet size is influenced differentially by the ratio of an emulsifier to a co-emulsifier (45). Each formulation had a PDI lower than 0.5, indicating a consistent and limited droplet size distribution (46).

Table 2. Thermodynamic stability study results

NE F-code	CEN. test	H&C cycles	F-T cycles
F1	√	√	√
F2	√	√	√
F3	√	X	-----
F4	√	√	√
F5	√	√	√
F6	√	√	√
F7	√	X	-----
F8	√	√	√
F9	√	√	√
F10	√	√	√
F11	√	√	√
F12	√	X	-----
F13	√	√	√
F14	√	√	√
F15	√	√	√
F16	√	√	√
F17	√	√	√
F18	√	X	-----
F19	√	√	√
F20	√	√	√

*Pass expressed as √, failed expressed as X, heating, and cooling termed (H&C), centrifugation termed as (CEN), and freeze-thaw termed as (F&T).

Table 3. The average droplet size, PDI, %T, and drug content (mean ± SD, n= 3)

NE F- code	OA (w/w) %	S-mix Ratio	S-mix (w/w) %	Particle size (nm)	Polydispersity Index	Light transmittance %	Drug Content %
F1	7	1:1	40	146.7±0.02	0.268±0.01	98.7±0.001	96±0.6
F2	10	1:1	50	150.1±0.01	0.3823±0.0	97.7±0.003	99±0.5
F4	20	1:1	50	162.2±0.012	0.2719±0.0	93.1±0.002	99.9±0.45
F5	25	1:1	55	170 ±0.02	0.39±0.01	94±0.002	95±0.5
F6	7	2:1	40	140.2±0.01	0.2278±0.0	97.1±0.001	95.2±0.4
F8	15	2:1	55	148±0.02	0.2317±0.01	95.8±0.002	100±0.5
F9	20	2:1	55	154±0.01	0.2464±0.01	95±0.001	94±0.4
F10	25	2:1	55	164±0.01	0.2032±0.0	94.2±0.002	95±0.4
F11	7	3:1	40	114.1±0.02	0.2137±0.01	99.04±0.003	99.8±0.45
F13	15	3:1	55	119.9±0.0	0.253±0.012	98.6±0.004	100±0.1
F14	20	3:1	55	125±0.012	0.246±0.01	97.8±0.003	100±0.32
F15	25	3:1	55	135 ±0.01	0.288±0.0	97±0.001	100±0.4
F16	7	1:2	53	125.8±0.02	0.285±0.01	97.9±0.002	100±0.0
F17	10	1:2	50	129.7±0.01	0.232±0.01	97.7±0.006	100±0.0
F19	20	1:2	55	133.3±0.02	0.245±0.01	97.6±0.001	100±0.5
F20	25	1:2	50	163.2±0.03	0.198±0.02	94.6±0.04	96±0.4

Measurement of transmitted light percentage (T%)

All NE formulations are conspicuous and influential light transmitters, as shown in Table 3, where the transmission percentage is close to 100%⁽⁴⁷⁾.

Predicted medication content

None of the developed formulations had medication residue since they all complied with British pharmacopeia standards and were within an acceptable range (95.0%-105.0%). More than 95% of the medication was present in all developed LSM NEs, as shown in Table 3. There was no significant difference between them ($p > 0.05$).

Test for dilution

The physical stability of the LSM NE has been demonstrated, even when diluted with DD. All NE formulations (F1-F20) manifested clear with a light sky-blue color in less than a minute, showing that they were of the o/w type and could be diluted in nasal secretions without drug deposition while still being nanoscale⁽⁴⁸⁾.

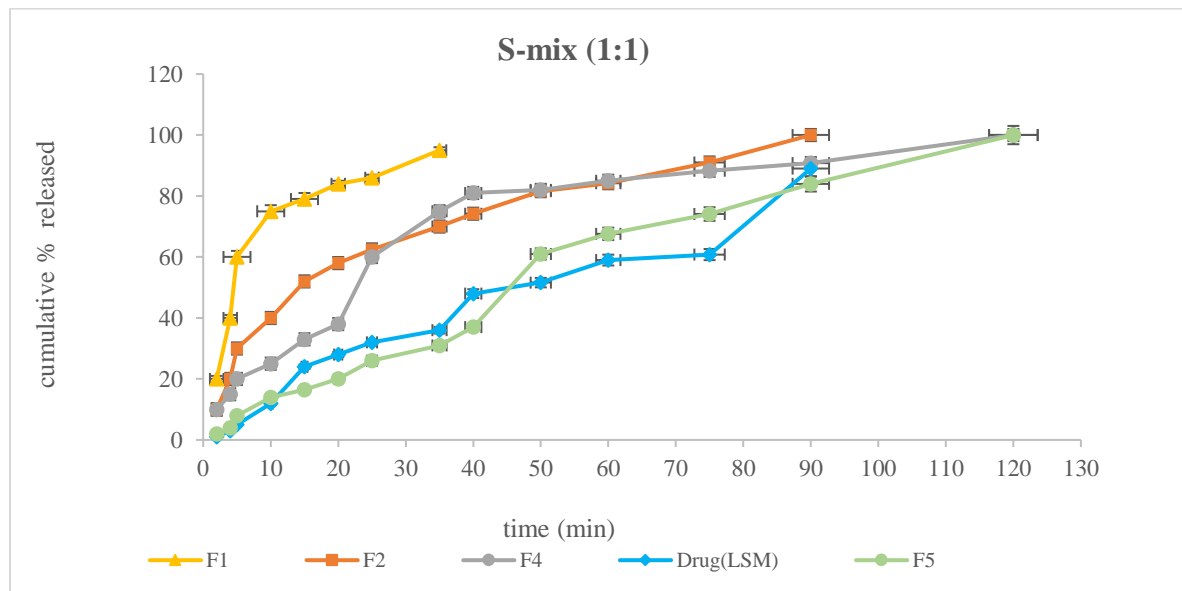
Drug release analysis in vitro

Due to its poor water solubility (1.0-3.56 mg/ml at 25 and 37 °C, respectively), the pure drug (LSM) released 32% after 25 minutes, which is noticeably less ($p < 0.05$) than the drug released from multiple NEs (F1, F6, F13, and F16), which is nearly 100%, as illustrated in Figure 4 below. The quantitative release of the medicine from an NE formulation is influenced by the size of the droplets⁽⁴⁹⁾. Droplet

size was increased, and the LSM cumulative percentage released was significantly decreased ($p < 0.05$) as the OA concentration increased for each S-mix ratio of the phase diagram. F1, F6, F13, and F16 represent the optimum formulas with the maximum release for S-mix 1:1,2:1,3:1, and 1:2 respectively⁽⁴³⁾.

At lower OA concentrations for different S-mix formulas (F1, F6, and F13), droplet sizes decrease (146.7, 140, 119.9 nm, respectively) accompanied by a higher cumulative percentage released (86, 90, and 100% at the end of 25 min) with an increase in LR concentration. These outcomes may be due to the surface activity of LR and its solubilization ability. Since LR lowered the interfacial tension between the oil and water phases, making the interface more fluid could lead to deeper oil penetration in the hydrophobic region of the LR monomers and, ultimately, a smaller droplet diameter⁽⁴⁴⁾.

Co-emulsifiers are good in solubilizing and aiding the dissolving process of the pure medication⁽⁵⁰⁾, and as demonstrated in F16, increasing the TC concentration causes the viscosity to drop and the release rate to increase up to 100% after 15 minutes. Figure 4 shows the release profile of NE formulations, which reveals that the best formulae (F1, F6, and F13) achieve a maximum release in 25 minutes, whereas F16 achieves the same result at the end of 15 minutes.



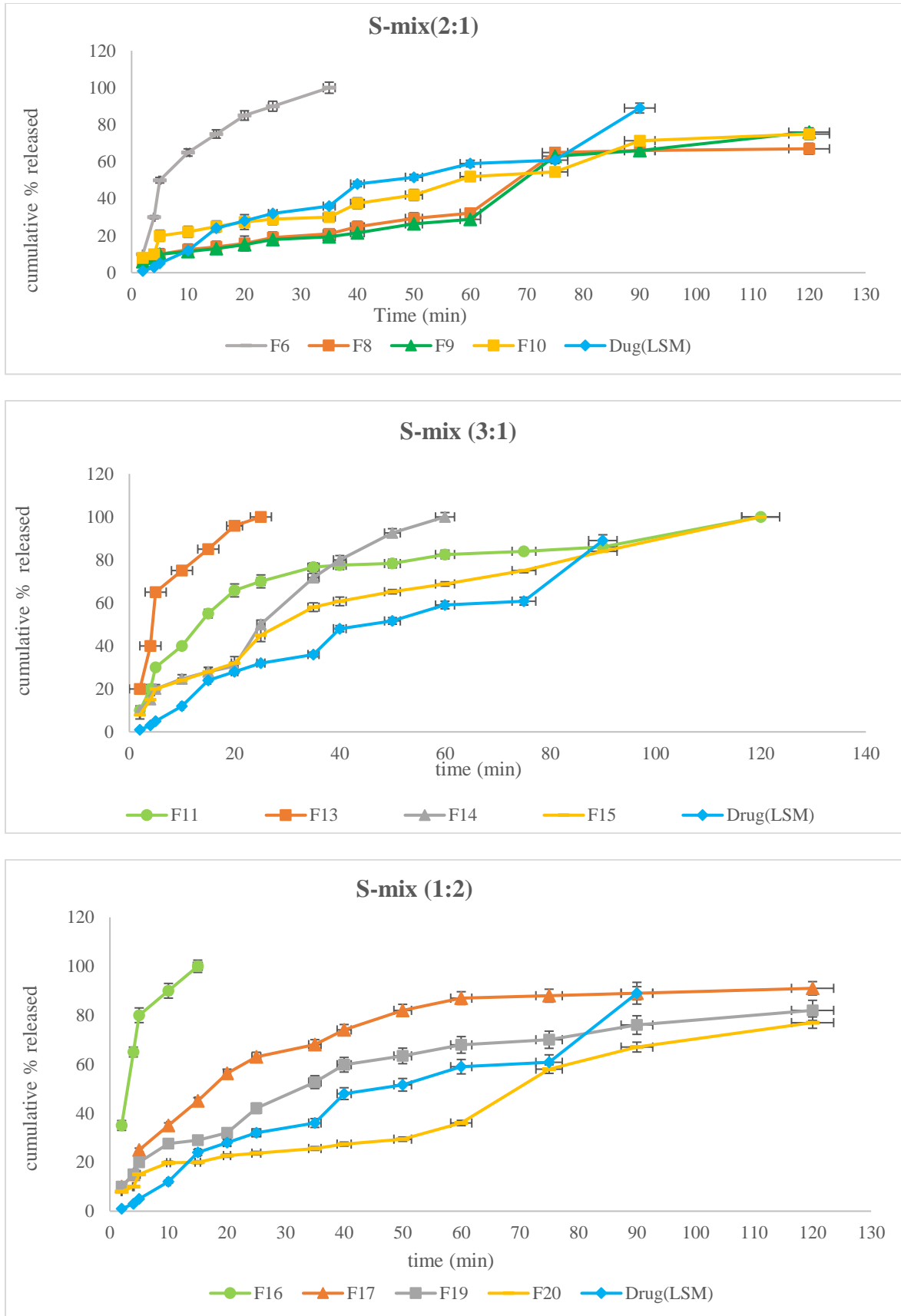


Figure 4. The S-mix: oil ratio influences the LSM NE and pure medication release profiles.

Choosing the best formulas for LSM NEs

Formulae F1, F6, F13, and F16 were selected as the best formulae based on the results of the characterization research of the produced NEs. It asserted the superiority of these formulations in terms of drug content, droplet size, PDI, and T%. Except for F16, which displays 100% release within just 15 minutes, all the optimal chosen NEs exhibit high with a quick release of LSM within 25 minutes. More research on the streamlined recipes would be made available.

Ex-vivo modeling of permeation analysis

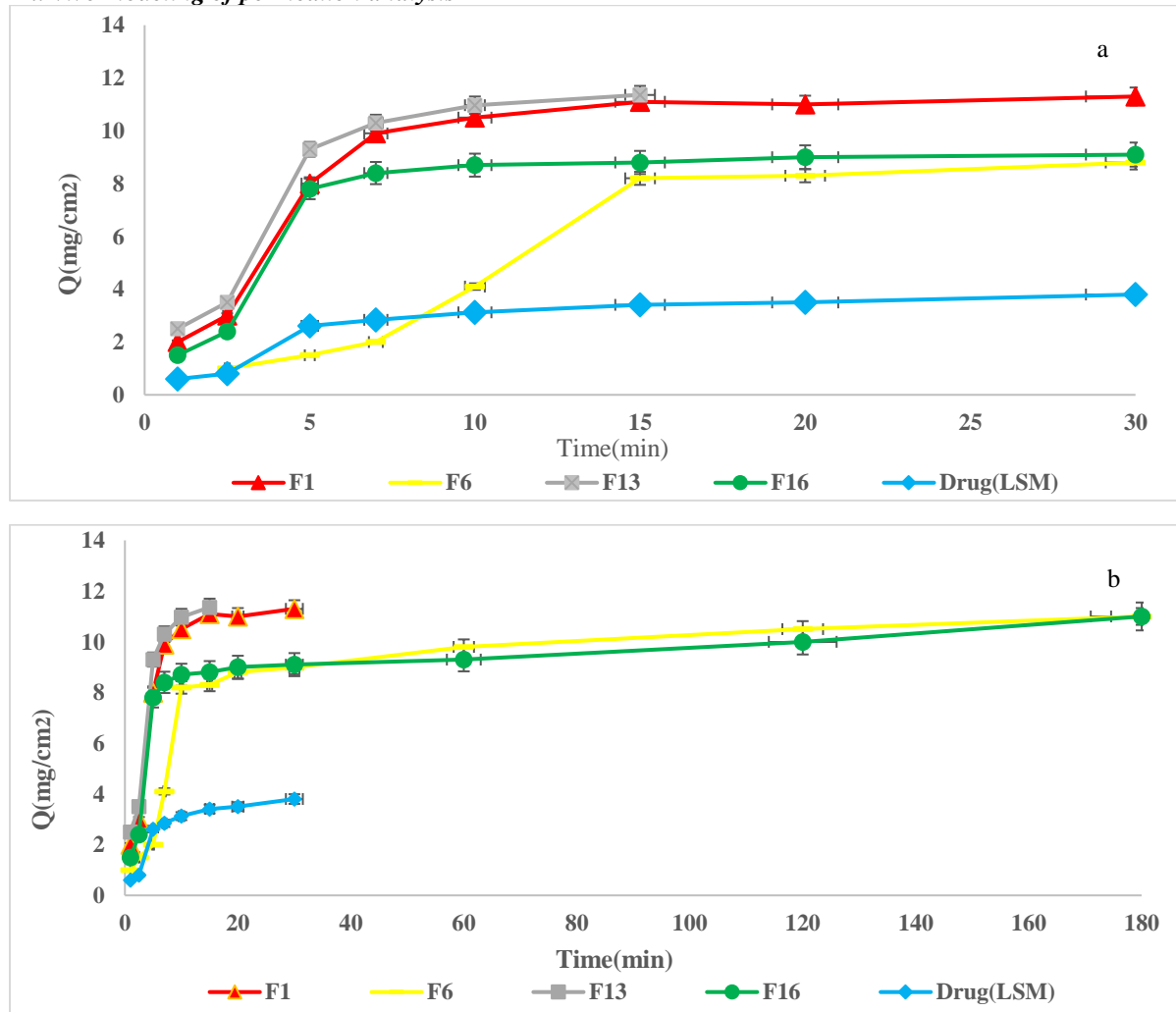


Figure 5. Ex-vivo permeation of the selected NEs formulas with LSM, a. For 30 min duration, and b. For three h (180 min) duration.

The results indicated that LSM from NEs-selected formulae would permeate significantly better than pure medication (aqueous LSM suspension), with a p-value of less than 0.05. This may be due to the fact that NEs persist intact in nasal tissue, where they can disrupt both lipid and polar permeation channels. In addition, the outer layer of nasal tissue can be more effectively moistened by the hydrophilic domain of NEs, improving medication absorption. As the aqueous fluid of the NEs moves along the polar channel, it disrupts the

Ex-vivo permeation studies were performed using fresh sheep nasal mucosa placed on the receptor portion of the Franz diffusion cell. Different NE formulations F1, F6, F13, F16, and pure drug (LSM 8%) as aqueous drug suspension were evaluated in the experiment.

The optimized NEs (F1, F6, and F16) achieved almost 100% permeation into the nasal mucosa of sheep at 0.5, 3, and 3 hours, respectively, as shown in Figures 5(a) and (b). Still, only F13 achieved 100% permeability after 15 minutes, whereas the pure drug exerted only 30%.

interfacial structure of the tissue lipid bilayer, increasing the volume between the lipid bilayer's lamellae⁽⁵¹⁾. The smaller globules in this formulation also allow for faster absorption⁽⁵²⁾. In addition, oleic acid enhances membrane permeability by activating lipophilic permeation⁽⁵³⁾.

Table 4 displays the permeation characteristics of NE formulations F1, F6, F13, and F16 compared to the control (LAS 8% as aqueous suspension). F13 outperforms the control regarding the flux and

permeation despite being formed as NIG with varying concentrations of Carbopol 934 (0.2, 0.5, and 0.7%).

Table 4. Ex-vivo permeation parameters

NE F- code	Lag time (min)	Flux (J)- (mg/cm ² .min)	P=J/Cd*10 ⁻² (cm/min)
F1	0.8	2	2.5
F6	4	1.24	1.55
F13	0.5	2.32	2.9
F16	1.8	2.16	2.7
Drug-LSM	2	0.724	0.91

In-vitro evaluation of NIGs

Table 5 below shows the results of an *in vitro* evaluation of the prepared NIG I, II, and III with 0.2, 0.5, and 0.7% Carbopol-934, respectively.

The evaluations included pH, gelling capacity, viscosity, and gel strength. The results were compared with those of NE (F13) and the corresponding emulsion-in situ gel (EMI).

Table 5. The pH, gelling capacity, gel strength, and viscosities (using spindel no.4 at 30 rpm) of NE(F13), NIGs (I, II& III), and EMI of LAS (mean ± SD, n= 3).

Formula code	pH	Gelling capacity	Viscosity Before gelation (mPa.s)	Viscosity after gelation (mPa.s)	Gel strength(s)
NEIG-1	6.2±0.01	+	2149±1.2	2593±1.5	19±0.2
NEIG-2	6.1±0.002	++	2560±2.0	3122±2.5	28±0.1
NEIG-3	5.9±0.005	+++	2615±1.6	3493±2.1	54±0.4
EMI	5.5±0.02	+	569±1	757±1.5	17±0.5
NE (F13)	6.7 ±0.01	-----	2120±2.5	-----	-----

**Where: +: gelation within 10 s, and remain for several minutes, ++: gelation within 6s for specific periods, +++: gelation within 4s, but for more extended periods (stiffer gel).

The results indicated that all the prepared NIGs were clear and had pH values between 5.9-6.2, which is compatible with nasal mucosal pH. Table 5 shows that all the NIGs exhibited instantaneous gelation upon contact with the artificial nasal fluid (at pH 6.4), which can be attributed to its buffering capacity⁽⁵⁴⁾.

All formulations tested showed pseudoplastic shear thinning behavior, according to the viscosity measurements. Table 5 demonstrates a significant increase ($p < 0.05$) in the viscosity values of NGs (2593-3493mPa.s) at the nasal pH in comparison to the NIGs in solution (2149-2615mPa.s); this change was exclusively the result of the gel conversion, indicating the in-situ nature of all the prepared gels. These gels were liquid at room temperature but rapidly gelled upon contact with the physiological pH (6.4). Figures 6(a) and (b) display the rheological profile of the LAS NE in situ gelling systems before and after gelation, respectively, and illustrate that the viscosity decreases with increasing angular velocity or shear rate⁽⁵⁵⁾.

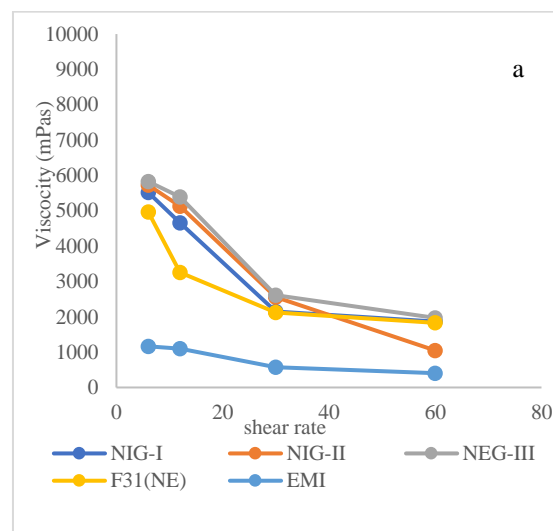


Figure 6. Rheological evaluation of the examined NIG (I- III) and EMI, a) Before gelation.

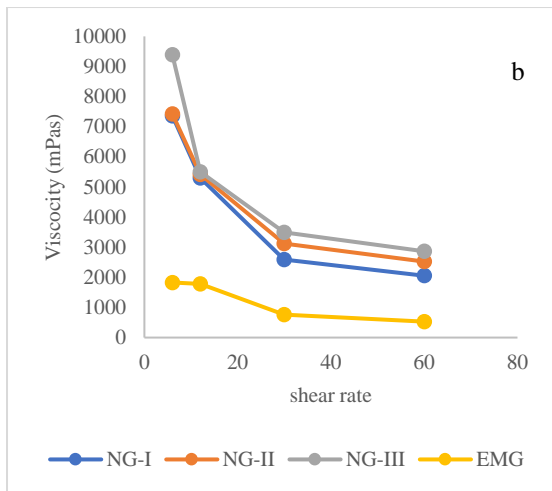


Figure 6. Rheological evaluation of the examined NIG (I- III) and EMI, b) after gelation.

Gel strength is an essential consideration for developing nasal administration systems because it allows for easy gel administration while limiting gel leakage, so it is a vital factor for developing a NIG. A suitable gel strength must be incorporated into the formulation for the nasal gel to be effective. While gels with a strength of 25 seconds (s) may not have enough structural integrity and may disintegrate soon⁽¹⁴⁾, gels with a strength of > 50 s may be too stiff (hard) and unpleasant to use. Due to their calculated values of gel strengths, NIG-I and NIG-III (19 and 54 s, respectively) were not included in the subsequent tests, leaving just NIG-II for further consideration.

In-vitro release / Ex-vivo permeation studies

Only NIG-II was subjected to *in-vitro* release and *ex-vivo* permeation. The results were compared with F13, EMI, and control (8% LSM as aqueous suspension), as shown below in Figures 7 (a and b).

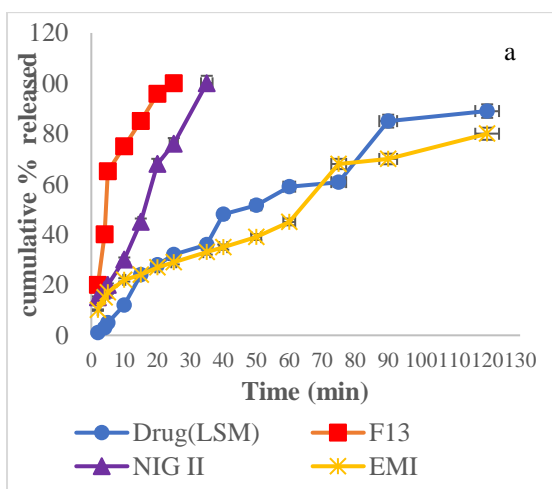


Figure 7.a) represents the *In-vitro* release study.

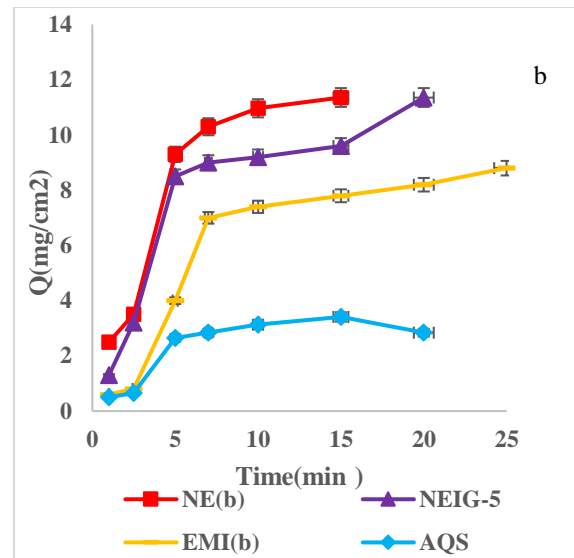


Figure 7. b) represents the *Ex-vivo* permeation study.

Complete permeation and release of NIG-II occurred at 20 and 35 minutes, respectively, according to the results. Adding 0.5% of Carbopol-934, a pH-induced gelling polymer commonly used to extend the residence duration of drugs, may alleviate the leakage issue even though NE(F13) shows quicker penetration and release⁽⁵⁶⁾.

The permeation parameters include Lag time, which is equal to **0.5, 1, 1.5, and 2 min**, and the steady-state flux value that was calculated from the slope of the ascending permeation line resulting from graphing Q versus time is equal to **2.32, 2.12, 1.38, and 0.724 mg/cm²min**. Finally, by dividing the calculated flux value over the initial LSM concentration (C_0) in the donor compartment, we can determine the permeability coefficient (P - value), which is equal to (2.9, 2.65, 1.73, and 0.9) $\times 10^{-2}$ **cm/min**, for NIG-II, F13, EMI, and control respectively.

The *ex-vivo* permeation data showed that NIG-II significantly improved the nasal permeation of LSM ($p < 0.05$), resulting in a 3.3-fold more significant penetration percentage accompanied by more residence time in the nasal cavity due to the high viscosity value Compared to an aqueous drug suspension (8% LSM) and EMI⁽⁵⁷⁾.

Surface morphology of NE using TEM

The shape and surface morphology of the optimized NE formulation F13 were studied using transmission electron microscopy, as shown in Figure 8. The TEM picture of the intranasal NE showed a spherical shape nanosized globule. The diameter of the droplet was found to be around 119-120 nm^(58,59).



Figure 8. Transmission electron microscopy of optimized NE (F13).

Conclusion

Based on the results obtained from this study, it can be concluded that LSM was successfully prepared as a nasal NIG, a new drug delivery strategy, which significantly enhanced ($p < 0.05$) the nasal permeation leading to a **3.3-fold** higher permeation percentage compared with an aqueous drug suspension (8% LAS) and about one and a half-fold compared with EMI. The modified nasal NIG formula contained 15% OA, 55% CE, and TC combined in a (3:1) S-mix ratio. A half percentage of Carbopole-934 was used as an in-situ gelling polymer to gel the chosen NE formula. NIG-II formula is a viable option for improving intranasal preparation efficacy. It exerts an excellent permeation with more residence time. This combination can address the primary issues with the oral LSM tablet. However, it won't eliminate the need for further clinical trials of this novel formula, which may provide doctors with additional essential details.

Acknowledgment

The authors thank the Department of Pharmaceutics, College of Pharmacy, University of Baghdad, for completing the research.

Conflicts of Interest

There are no conflicts of interest regarding the publication of my research article.

Funding

The researcher hasn't received any financial support from any institution except my college.

Ethics Statements

I would already get ethical approval from my college with the No: [REACUBCP2542022A](#).

Author Contribution

We certify that we have participated sufficiently in the intellectual content, conception, and design of this work, the analysis and interpretation of the data, and the writing of the manuscript to take public responsibility. We have agreed to have our name listed as a contributor. We

believe the manuscript represents valid work and approved the final revision of the manuscript.

References

1. Beauchene JK, Levien TL. Lasmiditan: Acute Migraine Treatment Without Vasoconstriction. A Review. *J Pharm Technol.* 2021; 37(5): 244–53.
2. Mecklenburg Jasper, et al. The potential of lasmiditan in migraine. *Ther. Adv. Neurol. Disord.* 2020; 13:1-11.
3. REYVOW (Lasmiditan) Tablets, Eli Lilly and Company. Available online: https://www.accessdata.fda.gov/drugsatfda_docs/label/2019/211280s0001bl.pdf (accessed on 30 June 2020).
4. Ramirez AL, Beltran ER, Haanes KA, Chan KY, Garrelds IM, Johnson KW, et al. Lasmiditan inhibits calcitonin gene-related peptide release in the rodent trigeminovascular system. *Pain.* 2020; 161(5): 1092–99.
5. Fiedler DS. Pharmacokinetics, pharmacodynamics, and drug–drug interactions of new anti-migraine drugs—Lasmiditan, gepants, and calcitonin-gene-related peptide (CGRP) receptor monoclonal antibodies. *Pharmaceutics.* 2020;12(12), 1180.
6. Korani S, Bahrami S, Korani M, Banach M, Johnston TP, Sahebkar A. Parenteral systems for statin delivery. *Lipids Health Dis.* 2019;18:193.
7. Sabri LA, Hussein AA. Oral liquid self-nanoemulsion of nebivolol: formulation and in-vitro characterization for dissolution rate enhancement. *IJDDT.* 2021;11(3):1083-91.
8. Elshafeey AH, Kamel AO, Fathallah MM. Utility of nanosize nanoemulsion for transdermal delivery of tolterodine tartrate: ex-vivo permeation and in-vivo pharmacokinetic studies. *Pharm Res.* 2009; 226:2446-53.
9. Huang C, Wang C, Zhang W, Yang T, Xia M, Lei X, et al. Preparation, in vitro and in vivo evaluation of nanoemulsion in-situ gel for transnasal delivery of traditional chinese

- medicine volatile oil from ligusticum sinense oliv. cv. chaxiong. *Molecules*.2022;27(21): 7644.
10. Abdulla N A, Balata G F, El-Ghamry H A, Gomaa E. Intranasal delivery of Clozapine using nanoemulsion-based in-situ gels: an approach for bioavailability enhancement. *Saudi Pharm J*. 2021;29(12):1466-1485.
 11. Fadhel AY, Rajab NA. Tizanidine intranasal nanoemulsion in-situ gel: formulation and in-vivo brain study. *J. Pharm. Negat*.2022;13(2): 582-591.
 12. Barbara V, et al. Recent advances in the development of in situ gelling drug delivery systems for non-parenteral administration routes. *Pharmaceutics*, 2020; 12(9): 859.
 13. Chakrabarty S, Nath B. Oral in-situ gel for periodontitis: A review. *World j. Pharm res*.2018;7(11):262-76.
 14. Hosny KM, Banjar ZM. The formulation of a nasal nanoemulsion zaleplon in situ gel for the treatment of insomnia. *Expert opinion on drug delivery*. 2013;10(8):1033-41.
 15. Khames A. Formulation and characterization of eplerenone nanoemulsion liquid solids, an oral delivery system with higher release rate and improved bioavailability. *Pharmaceutics*. 2019;11(1):18.
 16. Kumar R, Puppala K, Lakshmi V. Optimization and solubilization study of nanoemulsion budesonide and constructing pseudo ternary phase diagram. *Asian J Pharm Clin Res*.2019; 12 (1): 551-53.
 17. Almajidi YQ, Mahdi ZH, Maraie NK. Preparation and in vitro evaluation of montelukast sodium oral nanoemulsion. *Int J App Pharm*. 2018; 10 (5): 49-53.
 18. Suminar MM, Jufri M. Physical stability and antioxidant activity assay of a nanoemulsion gel formulation containing tocotrienol. *Int J App Pharm*.2017;9(1):140-3.
 19. Patel HC, Parmar G, Seth AK, Patel JD, Patel SR. Formulation and evaluation of o/w nanoemulsion of ketoconazole. *PSM*. 2013;4(4):338-51.
 20. Moghimipour E, Salimi A, Yousefvand T. Preparation and evaluation of celecoxib nanoemulsion for ocular drug delivery. *Asian J. Pharm*. 2017; 11 (3):543-50.
 21. Mohamadi SS, Abdolalizadehb J, Herisa SZ. Ultrasonic/sonochemical synthesis and evaluation of nanostructured oil in water emulsions for topical delivery of protein drugs. *Ultraso-Sonochem*.2019; 55:86–95.
 22. Patel G, Shelat P, Lalwani A. Statistical modeling, Optimization and characterization of solid self-nano emulsifying drug delivery system of lopinavir using design of experiment. *Drug Deliv*. 2016; 23(8):3027- 42.
 23. Mundada VP, Sawant KS. Enhanced oral bioavailability and anticoagulant activity of dabigatran etexilate by self-micro emulsifying drug delivery system: Systematic Development, in vitro, ex vivo and in vivo evaluation. *J Nanomed Nanotechnol*. 2018; 9(1):1-13.
 24. Alshahrani SM. Anti-inflammatory studies of ostrich oil-based nanoemulsion. *J Oleo Sci*.2019; 208(3):203–8.
 25. Pratiwi L, Fudholi A, Martien R, Pramono S. Design and Optimization of self-nano emulsifying drug delivery systems (SNEDDS) of ethyl acetate fraction from mangosteen peel (*Garcinia mangostana*, L.). *Inter J of PharmTech Res*. 2016;9(6): 380-87
 26. Maraie NK, Almajidi YQ. Application of nanoemulsion technology for preparation and evaluation of intranasal mucoadhesive nano-in-situ gel for ondansetron HCl. *J. Glob. Pharma Technol*. 2018; 10(03): 431- 4.
 27. Edresi S, Baie S. Formulation and stability of whitening VCO-in-water nano-cream. *Int. j. of pharmaceutics*. 2009;373(48):174-8.
 28. Baloch J, Sohail MF, Sarwar HS, Kiani MH, Khan GM, Jahan S, et al. Self-Nanoemulsifying Drug Delivery System (SNEDDS) for Improved Oral Bioavailability of Chlorpromazine: In Vitro and In Vivo Evaluation. *Medicina*. 2019;55(5):1-13.
 29. Bayanati M, Khosroshahi AG, Alvandi M, Mahboobian MM. Fabrication of a thermosensitive in situ gel nanoemulsion for nose to brain delivery of temozolomide. *J. Nanomater*. 2021: 1-11.
 30. Ahmad N, Ahmad R, Buhezaha TM, AlHomoud HS, Al-Nasif HA, Sarafroz MD. A comparative ex vivo permeation evaluation of a novel 5-Fluorouracil nanoemulsion-gel by topically applied in the different excised rat, goat, and cow skin. *Saudi J Biol Sci*. 2020;7: 1024–40.
 31. Abdulla NA, Balata GF, El-Ghamry HA, Gomaa E. Intranasal delivery of Clozapine using nanoemulsion-based in-situ gels: An approach for bioavailability enhancement. *Saudi Pharm J*. 2021;29(12):1466-85.
 32. Ameen D, Michniak-Kohna B. Transdermal delivery of dimethyl fumarate for Alzheimer's disease: Effect of penetration enhancers. *Inter of Pharm*. 2017; 529, 465–73.
 33. Bhalerao H, Koteswara KB, Chandran S. Design, Optimization and evaluation of in situ gelling nanoemulsion formulations of brinzolamide. *Drug Deliv. Transl. Res*. 2020;10: 529-47.
 34. Kolsure PK, Raj Kapoor B. Development of zolmitriptan gel for nasal administration. *Asian J Pharm Clin Res*. 2012; 5:88-94.
 35. Alkufi HK, Kassab HJ. Formulation and evaluation of sustained release sumatriptan

- mucoadhesive intranasal in-situ gel. *Iraqi J Pharm Sci.* 2019;28(2):95-104.
36. Rajaa A D, Nawal AR. Formulation and investigation of lacidipine as nanoemulsions. *Iraqi J Pharm Sci.* 2020;29(1):41-45.
 37. Da Costa S, Basri M, Shamsudin N, Basri H. Stability of Positively Charged Nanoemulsion Formulation Containing Steroidal Drug for Effective Transdermal Application. *J. Chem.* 2014:1-9.
 38. Kaur G, Singh P, Sharma S. Physical, morphological, and storage studies of cinnamon-based nanoemulsions developed with Tween 80 and soy lecithin: A comparative study. *J. Food Meas. Charact.* 2021;15: 2386–98.
 39. Morsi N, Ibrahim M, Refai H. Nanoemulsion-based electrolyte triggered in situ gel for ocular delivery of acetazolamide. *Eur. J Pharm Sci.* 2017;104: 302-14.
 40. Misra SK, Pathak K. Nose-to-Brain Targeting via Nanoemulsion: Significance and Evidence. *J. Colloid Interface Sci.* 2023; 7(1):23.
 41. Kawakami K, Yoshikawa T, Moroto Y, et al. Microemulsion formulation for enhanced absorption of poorly soluble drugs I. Prescription design. *J Control Release* 2002; 81:65-74.
 42. Hanifah M, Jufri M. Formulation and stability testing of nanoemulsion lotion containing *Centella asiatica* extract. *J Young Pharm.* 2018;10(4):404–8.
 43. An Y, Yan X, Li B, Li Y. Microencapsulation of capsanthin by self-emulsifying nanoemulsions and stability evaluation. *Eur. Food Res. Technol.* 2014; 239:1077–85.
 44. Sarheed O, Dibi M, Ramesh K. studies on the effect of oil and surfactant on the formation of alginate-based o/w lidocaine nanocarriers using nanoemulsion template. *pharmaceutics.* 2020 ;12(12):1223.
 45. Sadoon NA, Ghareeb MM. Formulation and Characterization of Isradipine as Oral Nanoemulsion. *Iraqi J Pharm Sci.* 2020;29(1):143-15.
 46. Hadi AS, Ghareeb MM. Rizatriptan benzoate nanoemulsion for intranasal drug delivery: preparation and characterization. *IJDDT.*2022;2 (2) :546-52.
 47. Drais HK, Hussein AA. Formulation and characterization of carvedilol nanoemulsion oral liquid dosage form. *Int J Pharm Pharm Sci.* 2015;7(12):209-16.
 48. Al-sakini SJ, Maraie NK. Optimization and in vitro evaluation of the release of class II drug from its nanocubosomal dispersion. *Int J Appl Pharm.* 2019;11(2):86–90.
 49. Hamed SB, Alhammid SNA. Formulation and Characterization of Felodipine as an Oral Nanoemulsion. *Iraqi J Pharm Sci.* 2021;30(1):209–217.
 50. Pandya D, Rana B, Solanki N. Oral bioavailability enhancement of bromocryptine mesylate by self-micro emulsifying drug delivery system (smedd). *int j pharm pharm sci.*2016; 8(6):76-81.
 51. Baboota S, Shakeel F, Ahuja A, Ali J, Shafiq S. Design, development and evaluation of novel nanoemulsion formulations for the transdermal potential of celecoxib. *Acta Pharmaceutica.* 2007; 57(3): 315-32.
 52. Mahajan HS, Mahajan MS, Nerkar PP, Agrawal A. Nanoemulsion-based intranasal drug delivery system of saquinavir mesylate for brain targeting. *Drug Deliv.* 2014;21(2):148–54.
 53. Patel MR, Patel MH, Patel RB. Preparation and in vitro/ex vivo evaluation of nanoemulsion for transnasal delivery of paliperidone. *Appl Nanosci.* 2016;6(8):1095–104.
 54. Sulaiman HT, Jabir SA, Al-kinani KK. Investigating the effect of different grades and concentrations of pH-sensitive polymer on preparation and characterization of lidocaine hydrochloride as in situ gel buccal spray. *Asian J Pharm Clin Res.*2018; 11(11):1-7.
 55. Patil S, Kadam A, Bandgar S, Patil SH. formulation and evaluation of an in-situ gel for ocular drug delivery of anti-conjunctival drug. *Cellulose Chem. Technol.* 2015;49 (1): 35-40.
 56. Nief RA, Tamer MA, Abd Alhammid SHN. Mucoadhesive oral in situ gel of itraconazole using pH-sensitive polymers: Preparation, and in vitro characterization, release, and rheology study. *Drug Invent. Today.* 2019; 11(6):1450-55.
 57. Jaber SH& Rajab NA. Lasmiditan nanoemulsion based in situ gel intranasal dosage form: formulation, characterization and in vivo study. *Farmacia.*2023; 71(6):1241-53.
 58. Changediya VV, Jani R, Kakde P. A Review on Nanoemulsions: A Recent Drug Delivery Tool. *J Drug Deliv. Ther.* 2019; 9(5):185-91.
 59. Prajapati BG, Patel AG, Paliwal H. Fabrication of nanoemulsion-based in situ gel using moxifloxacin hydrochloride as a model drug for the treatment of conjunctivitis. *Food Hydrocoll.*2021;1:7.